ROBUST YAW CONTROL DESIGN WITH ACTIVE DIFFERENTIAL AND ACTIVE ROLL CONTROL SYSTEMS

Johannes Gerhard, Maria-Christina Laiou, Martin Mönnigmann, Wolfgang Marquardt
Lehrstuhl für Prozesstechnik, RWTH Aachen University
Templergraben 55, D-52056 Aachen, Germany
E-mail: gerhard@lpt.rwth-aachen.de

Mohsen Lakehal-Ayat, Edo Aneke, Rainer Busch
Ford Forschungszentrum Aachen, Ford Motor Company
Süsterfeldstr. 200, D-52072 Aachen, Germany
E-mail: mlakehal@ford.com

Abstract: A simple robust yaw controller for the nonlinear single-track model is designed, making use of active differential and active roll control systems. Robustness is studied for uncertainties in several model parameters, namely the vehicle longitudinal velocity, the road adherence coefficients and the hand wheel angle. Constructive nonlinear dynamics are employed for the controller design. The controller parameters are selected by solving an optimization problem. Stability of the solution is guaranteed by constraints that ensure a minimal distance between the nominal operating point and a stability boundary in the space of uncertain parameters.

Keywords: Nonlinear dynamics, optimization, bifurcations, vehicle dynamics, yaw control, controlled differentials, active roll control.

1. INTRODUCTION

Active control systems are becoming increasingly common in modern vehicles. The aim of these systems is to enhance the driving dynamics while maintaining the stability of the system under parametric uncertainty. Parametric uncertainty arises both from varying driver inputs, e. g. the longitudinal velocity and the hand wheel angle, as well as varying environmental conditions, e. g. the road conditions. In most studies, e. g. (Ackermann *et al.* 2002, Güvenç *et al.* 2004), a linearized vehicle model is used for the control design, neglecting nonlinear phenomena that may arise when the uncertain parameters deviate from their assumed nominal values. Previous investigations (Ono *et al.* 1998) however show that vehicle models exhibit a saddle node bifurcation (Wiggins 1990), beyond which trajectories become divergent causing the vehicle to fall into spin.

In this work an optimization approach based on nonlinear dynamics theory (Mönnigmann and Marquardt 2002) is employed for the control design. This method ensures robust stability of the solution by enforcing a specified distance from a stability boundary in the space of uncertain parameters. The stability boundaries are derived from bifurcation theory and take the nonlinearities of the system into account. The nonlinear single-track model (Mitschke 1990) is used for the vehicle dynamics and a simple yaw rate control realized by both active differential and active roll control systems is considered. The nonlinear dynamics approach is used to find a controller setting that minimizes the tracking error for stationary cornering and guarantees vehicle stability

for varying road conditions, longitudinal velocity and hand wheel angle.

The paper is structured as follows. Section 2 briefly introduces the method used for the robust controller design and tuning. Section 3 discusses the vehicle model and the control structure. Section 4 presents the main results of the paper, namely the robust controller tuning for three different scenarios. Finally, section 5 discusses the obtained results and summarizes the main conclusions.

2. BACKGROUND

The problem studied in this work is the robust stabilization of an uncertain nonlinear system when the control law structure is given. The closed loop system is described by equations of the form

$$\dot{x} = f(x, \alpha, p)\,, \quad x(t_0) = x_0\,, \tag{1}$$

where $x \in \mathbb{R}^{n_x}$ denotes the state vector, $\alpha \in \mathbb{R}^{n_\alpha}$ the vector of the uncertain system parameters and $p \in \mathbb{R}^{n_p}$ the vector of the tunable control parameters. The function f is assumed to be sufficiently smooth with respect to x, α and p. Furthermore, it is assumed that the uncertain system parameters α vary within known ranges, i. e.

$$\alpha_i \in \left[\alpha_i^{(0)} - \Delta\alpha_i,\, \alpha_i^{(0)} + \Delta\alpha_i\right]\,,\; i = 1, \ldots, n_\alpha\,,$$

where $\alpha_i^{(0)}$ denotes the nominal value of the parameter α_i and $\pm\Delta\alpha_i$ its upper and lower uncertainty bounds.

Since the controller structure is given, the control design task is reduced to tuning the controller parameters, so that the closed loop system is stable under the parameter uncertainties. To this end, a recently presented approach (Mönnigmann and Marquardt 2002, Mönnigmann and Marquardt 2003) for process optimization in the presence of parametric uncertainty is employed. The basic idea of this approach is to utilize critical manifolds, e. g. stability boundaries, that separate the parameter space into regions where the equilibrium points of system (1) exhibit qualitatively different behavior. Another type of a critical manifold that could also be handled by this approach is boundaries in the complex plane limiting the real and imaginary parts of the eigenvalues of the linear approximation of system (1). The approach enforces a lower bound on the parametric distance between a nominal operating point $\alpha^{(0)}$ and the nearest point $\alpha^{(1)}$ on the critical boundary. This lower bound ensures that the complete range of the uncertain parameters is at a safe distance from the critical boundary. Note that, since this approach only considers steady states of system (1), the desired property of the operating point, e. g. stability, can only be guaranteed for variations of the uncertain parameters α that are slow compared to the time scale of the system. In other words, the parameters α may only vary quasistatically with respect to the system dynamics.

Figure 1 shows a critical boundary and the uncertainty region for $n_\alpha = 2$. The parameters have been normalized with their uncertainties $\Delta\alpha$. For

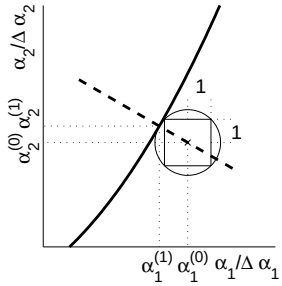

Fig. 1. Robust operating point $\alpha^{(0)}$ with stability boundary (thick line) and normal vector direction r (dashed thick line).

the normalized parameters $\alpha/\Delta\alpha$ the minimal distance between the nominal point $\alpha^{(0)}$ and the closest critical point $\alpha^{(1)}$ is equal to $\sqrt{n_\alpha}$. Since the shortest distance between $\alpha^{(0)}$ and $\alpha^{(1)}$ occurs along the direction of the normal vector r to the critical manifold (Dobson 1993), the robustness constraints can be stated as

$$\begin{aligned} \alpha^{(0)} &= \alpha^{(1)} + l\frac{r}{\|r\|} \\ l &\geq \sqrt{n_\alpha}\,. \end{aligned} \tag{2}$$

The normal vector r can generally be computed by a system of equations of the form

$$0 = G(x^{(1)}, \tilde{x}, p^{(0)}, \alpha^{(1)}, r)\,, \tag{3}$$

where $\tilde{x}$ denotes auxiliary variables. For a detailed description of $G(\cdot)$ the reader is referred to (Mönnigmann and Marquardt 2002).

Conditions (2) and (3) must hold in order to guarantee robust stability within the specified range of parametric uncertainty. Furthermore, if additionally a cost function ϕ is given, a robust optimum of system (1) with respect to ϕ can be found by solving the following constrained nonlinear program

$$\min_{x^{(0)},\alpha^{(0)},p^{(0)}} \phi(x^{(0)}, \alpha^{(0)}, p^{(0)}) \tag{4a}$$

$$\text{s. t.} \quad 0 = f(x^{(0)}, \alpha^{(0)}, p^{(0)})\,, \tag{4b}$$

$$0 = G(x^{(1)}, \tilde{x}^{(1)}, \alpha^{(1)}, p^{(0)}, r)\,, \tag{4c}$$

$$0 = \alpha^{(1)} - \alpha^{(0)} + l\frac{r}{\|r\|}\,, \tag{4d}$$

$$0 \leq l - \sqrt{n_\alpha}\,. \tag{4e}$$

3. VEHICLE MODEL

The nonlinear single-track model (Mitschke 1990) is utilized for the control design, while the actu-

ator dynamics are ignored. The tyre model presented by Pacejka and Bakker (1991) is used. Two body controllers are employed, namely a yaw controller and a roll controller. The closed loop system is depicted in Figure 2.

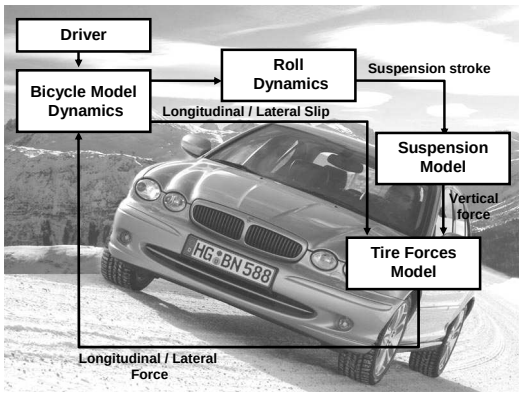

Fig. 2. Vehicle model

3.1 State space model

The equations of motion for each degree of freedom are

$$m(\dot{V}+Ur) = \mu_1 F_{y1}+\mu_2 F_{y2}+\mu_3 F_{y3}+\mu_4 F_{y4}\,, \quad (5)$$

$$I_{zz}\dot{r} = b(\mu_1 F_{y1}+\mu_2 F_{y2}) - c(\mu_3 F_{y3}+\mu_4 F_{y4}) + T_r\,, \quad (6)$$

$$\ddot{\varphi} = \frac{1}{J_x}\left[-D_x\dot{\varphi} - \Phi_x\varphi + m_{\rm sp}a_y h_{\rm cg} + \sin(\varphi) g m_{\rm sp} h_{\rm cr}\right] + T_\varphi\,, \quad (7)$$

where m denotes the total vehicle mass, V and U the vehicle sideslip and longitudinal velocities, respectively, r the vehicle yaw rate, μ_i the road adherence coefficients, F_{yi} the lateral forces, I_{zz} the yaw moment of inertia, b and c the longitudinal distances between the center of mass and the front and rare axles, respectively, T_r the engine torque, J_x the inertia around the longitudinal axis, D_x the damping of the angle velocity, Φ_x the spring constant, φ the roll angle, $m_{\rm sp}$ the vehicle chassis mass, α_y the vehicle lateral acceleration, $h_{\rm cg}$ the height of the center of gravity, g the acceleration of gravity, $h_{\rm cr}$ the height of the center of roll and T_φ the roll torque.

3.2 Body controllers

Two body controllers are used, a yaw and a roll controller.

The aim of the yaw controller is to track a body yaw rate reference $r_{\rm ref}$, which is defined as a function of the longitudinal velocity U and the road steering angle δ_n

$$r_{\rm ref} = \frac{a_r U}{1+b_r U^2}\delta_n. \quad (8)$$

The road steering angle δ_n is mainly influenced by the hand wheel angle $\delta_{\rm hwa}$

$$\delta_n = K_\delta \delta_{\rm hwa} \quad (9)$$

where K_δ is a constant steering ratio. It is further assumed that the hand wheel angle is upper bounded by a function of the longitudinal velocity

$$\delta_{\rm hwa,max} = 160\frac{1+b_r U^2}{a_r U^2} \quad (10)$$

so that the lateral acceleration does not exceed the upper physical limit of the gravity acceleration.

The yaw body control law is a simple saturated P-controller

$$T_r = -{\rm sat}(K_r(r-r_{\rm ref})) \quad (11)$$

where

$${\rm sat}(x) = \begin{cases} x, & \text{if } |x| \le T_{\max} \\ T_{\max}\cdot{\rm sign}(x), & \text{elsewhere} \end{cases}. \quad (12)$$

Since, as mentioned in Section 2, the function f in system (1) should be sufficiently smooth, the saturation function (12) cannot be incorporated in its current form in the study. Therefore it has been approximated by a suitable smooth function.

The roll body controller is used for the implementation of active suspension and is defined by

$$T_\varphi = -\Phi_x\varphi_{\rm ref} - m_{\rm sp}a_y h_{\rm cg} - \sin(\varphi_{\rm ref}) g m_{\rm sp} h_{\rm cr}. \quad (13)$$

The reference signal $\varphi_{\rm ref}$ is given by

$$\varphi_{\rm ref} = K_\varphi\left(\frac{a_y}{g}\right)^3. \quad (14)$$

The parameter K_φ influences the driving comfort of the passengers. It is fixed at a typical value $K_\varphi = 0.05$ in all the results presented below.

The roll torque is actively distributed between the front and rear axles. The distribution factor λ may vary within the range $[0.15,\ 0.85]$. To incorporate the effect of the active suspension including roll torque and its distribution, the corner loads F_{zi} are calculated as

$$\begin{bmatrix} F_{z_{FL}} \\ F_{z_{FR}} \\ F_{z_{RL}} \\ F_{z_{RR}} \end{bmatrix} = \begin{bmatrix} \frac{1}{2}\frac{c}{b+c}mg + m_F g + (1-\lambda)\frac{T_\varphi}{s_f} \\ \frac{1}{2}\frac{c}{b+c}mg + m_F g - (1-\lambda)\frac{T_\varphi}{s_f} \\ \frac{1}{2}\frac{b}{b+c}mg + m_R g - \lambda\frac{T_\varphi}{s_f} \\ \frac{1}{2}\frac{b}{b+c}mg + m_R g + \lambda\frac{T_\varphi}{s_f} \end{bmatrix} \quad (15)$$

where m_F and m_R denote the front and rear axle vehicle mass, respectively and s_f the track width. As the corner loads F_{zi} govern the lateral forces F_{yi}, there is an indirect effect of λ and T_φ on the yaw rate r. Therefore λ is used here for yaw rate tracking by introducing a second P-controller

$$\lambda = \begin{cases} 0.15, & \lambda \le 0.15 \\ (1-\frac{\alpha_y}{g})K_\lambda(r_{\rm ref}-r)+0.5, & 0.15 < \lambda < 0.85. \\ 0.85, & \lambda \ge 0.85 \end{cases} \quad (16)$$

The saturation of λ is again approximated by an appropriate smooth function.

3.3 Model uncertainties

The robustness of the proposed control law is studied against variations of the following parameters:

- longitudinal velocity $U[m/sec]$: $U \in [15, 50]$;
- road adherence coefficients μ_1, μ_2, μ_3, $\mu_4 \in [0.1, 1.2]$;
- hand wheel angle $\delta_{\text{hwa}} \in [0, \delta_{\text{hwa,max}}]$.

For simplicity $\mu_1 = \mu_3 = \mu_l$ and $\mu_2 = \mu_4 = \mu_r$ is assumed in the following.

4. RESULTS

A number of different case studies have been considered. The aim in all case studies is to find a controller setting that

(1) minimizes the tracking error and
(2) guarantees stability for the ranges of uncertainties described in section 3.3.

Due to the symmetry of the vehicle model only positive steering wheel angles – equivalent to left turns – need to be considered. Minimization of the steady state yaw rate tracking error $r_{\text{ref}} - r$ is addressed by the objective function

$$\phi = (r_{\text{ref}} - r)^2 \tag{17}$$

of the optimization problem (4), where minimal distance constraints on the critical stability boundary ensure the requested robustness.

Ideally the controller setting found by the optimization should stabilize the vehicle for the entire range of parametric uncertainty as described in Section 3.3.

The following three case studies have been investigated:

(1) proportional yaw rate controller with tuning parameters K_r, $T_{\max}$ and K_λ;
(2) gain scheduling of the controller tuning in the longitudinal velocity U;
(3) gain scheduling of the controller tuning in the adherence coefficients μ_l, μ_r.

In all case studies lower and upper limits of the tuning parameters are set to $T_{\max}[\text{Nm}] \in [0, 2000]$, $K_r \in [0, 50000]$ and $K_\lambda \in [-100, 100]$.

In order to apply the optimization approach presented in Section 2, nominal values of the uncertain parameters have to be specified. A natural choice for the nominal values are the mean values of the uncertainty ranges

$$\mu_r^{(0)} = 0.65\,, \quad \mu_l^{(0)} = 0.65\,, \quad U^{(0)} = 32.5\,m/s\,.$$

For the hand wheel angle the worst case scenario $\delta_{\text{hwa}} = \delta_{\text{hwa,max}}$ is considered in all presented case studies.

Bifurcation analysis of the bicycle model shows that the dynamic behavior of the vehicle is dominated by a saddle node bifurcation, where a real eigenvalue of the linearized model crosses the imaginary axis. In Figure 3a steady state continuation in the road adherence coefficient μ_l reveals such a saddle node bifurcation for the nominal values of $U^{(0)} = 32.5\,m/s$ and $\mu_r^{(0)} = 0.65$. A critical manifold composed of saddle node bifurcations is obtained by varying a second parameter as shown in Figure 3b for μ_r.

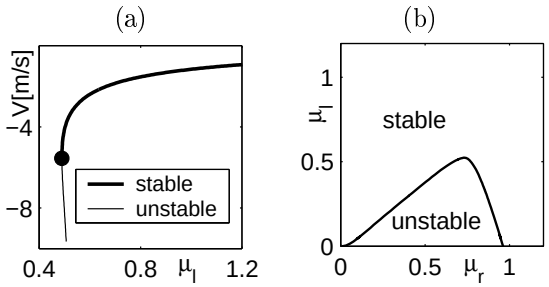

Fig. 3. (a) Equilibrium curve with saddle node bifurcation • and (b) critical manifold of saddle node points in the (μ_r, μ_l) parameter plane.

4.1 Case study 1

The first case study is the basis for the other two scenarios. Parametric robustness against loss of stability is ensured by normal vector constraints on the saddle node bifurcation. The solution of the optimization problem (4) reveals, however, that it is not possible to stabilize the vehicle for the entire range of uncertainty defined in Section 3.3, i. e. no operating point can be found that satisfies the robustness constraints (4c)–(4e). The optimization problem (4) is therefore modified and used to find the most robust controller setting. This is equivalent to maximizing the distance l between the nominal operating point $\alpha^{(0)}$ and the nearest critical point $\alpha^{(c)}$. The cost function (17) is therefore set to

$$\phi = -l \tag{18}$$

and the inequality constraint (4e) of the optimization problem (4) is omitted. The aim of minimizing the tracking error is completely neglected in this case study, giving way to the maximization of the parametric distance, i. e. of the robustness region.

Table 1. Case study 1

max. stability range		contr. setting		yaw rate	
U	$[15, 50]$	K_r	13497	$r^{(0)}$	0.15
μ_r	$[0.39, 0.91]$	$T_{\max}$	0	$r_{\text{ref}}^{(0)}$	0.33
μ_l	$[0.39, 0.91]$	K_λ	-50	r/r_{ref}	0.45

In Table 1 the solution of this reformulated optimization problem shows that the maximal range of the robustness region is achieved by a controller setting where the maximal output of the yaw rate

controller $T_{\max}$ is set to 0. Obviously, the greatest stability is achieved by the passive vehicle. As stated above, the objective of minimizing the tracking error is not addressed and r is 55% off the reference signal r_{ref} at the steady state. The results show that even for the passive vehicle the achieved robustness region is somewhat smaller than the originally requested range of uncertainties, especially for μ_l and μ_r. It can be concluded that the road adherence coefficients have a greater influence on the stability than the longitudinal velocity U. A comparison of the achieved and the requested range is shown in Figure 4.

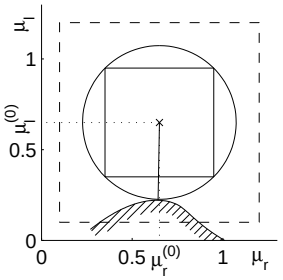

Fig. 4. Case study 1: The achieved range of stability (solid box) is smaller than the requested (dashed box).

Note that K_r has no influence on the stability if $T_{\max} = 0$. Loosely speaking, the high value of K_r is chosen arbitrarily by the NLP solver. The parameter K_λ of the control law (16) is tuned to a negative value. For the positive tracking error $r_{\text{ref}} - r$ this results in small values of λ, which corresponds to a shift of the roll torque to the front axis that has a stabilizing effect on the vehicle.

4.2 Case study 2

This case study investigates if relaxation of the requested robustness range in the longitudinal velocity U has a positive influence on the range of stability achieved for the road adherence coefficients μ_l and μ_r. This is equivalent to introducing gain scheduling in U. Three ranges $U_1 \in [15, 25]$, $U_2 \in [25, 40]$, $U_3 \in [40, 50]$ are considered. The influence though of the diminished ranges of U on the achieved ranges of stability for (μ_r, μ_l) turns out to be very small. These stability ranges are again smaller than those actually requested. Normal vector constraints are therefore used to maximize this region rather than guaranteeing stability of the optimized operating point for a specified range of uncertainty. As in the previous case, the passive vehicle with $T_{\max} = 0$ achieves the largest range of stability. The results obviously confirm the finding of the first case study that the longitudinal velocity is the less critical parameter.

4.3 Case study 3

The two previous case studies show that it is not possible to find a proportional controller that stabilizes the vehicle for the complete range of the uncertainties. Even the passive vehicle becomes unstable for some values inside the uncertainty region specified in Section 3.3, with the adherence coefficients μ_r, μ_l as the more critical parameters with respect to loss of stability. Therefore, in the third case study a different approach is proposed. A gain scheduling strategy for various ranges of μ is considered. It allows for the relaxation of the requested robustness ranges in these critical parameters. The following ranges and corresponding nominal operating points are studied

$$\begin{aligned} \mu_{r,1}^{(0)} = \mu_{l,1}^{(0)} &= 0.45\,, \mu_1 \in [0.3, 0.6] \\ \mu_{r,2}^{(0)} = \mu_{l,2}^{(0)} &= 0.75\,, \mu_2 \in [0.6, 0.9] \\ \mu_{r,3}^{(0)} = \mu_{l,3}^{(0)} &= 1.05\,, \mu_3 \in [0.9, 1.2]. \end{aligned} \tag{19}$$

These ranges of μ can be envisioned as three typical types of road conditions, the first representing an icy road, the second a wet road and the third a dry road. The range of U remains unchanged in comparison to the first case study. Clearly this approach requires measurement or reliable estimation of the road conditions. Several strategies for the estimation of the road friction have been suggested in the literature, see e. g. (Gustafsson 1997). It is, however, out of scope for this paper to discuss these approaches in detail. For simplicity we assume here that measurement of μ is available.

Table 2. Case study 3: icy road

max. stability range		contr. setting		yaw rate	
U	$[15, 50]$	K_r	50000	$r^{(0)}$	0.12
μ_r	$[0.3, 0.6]$	$T_{\max}$	0	$r_{\text{ref}}^{(0)}$	0.33
μ_l	$[0.3, 0.6]$	K_λ	-25	r/r_{ref}	0.36

The results of the optimization for the first operating point given in Table 2 show that the specified robust stability is achieved. As in the previous scenarios, the yaw torque is switched off by the optimization, in order to increase the robustness. This results again in a large difference between the yaw rate r and the reference signal r_{ref}.

Table 3. Case study 3: wet road

max. stability range		contr. setting		yaw rate	
U	$[15, 50]$	K_r	6483	$r^{(0)}$	0.23
μ_r	$[0.6, 0.9]$	$T_{\max}$	1506	$r_{\text{ref}}^{(0)}$	0.33
μ_l	$[0.6, 0.9]$	K_λ	12	r/r_{ref}	0.70

The results of the optimization for the second operating point for values of μ in the middle range between 0.6 and 0.9 are summarized in Table 3. Compared to all previous results a qualitatively different solution is obtained in this case. The reduced specified range of robustness allows for

a controller tuning that not only guarantees stability for the smaller range of uncertainty but also addresses the objective of minimizing the tracking error. In this case study the original optimization problem (4) and cost function (17) are used. In contrast to the previous results $K_r > 0$ and $T_{\max} > 0$, which means that yaw torque is used for yaw rate control. The switched sign of K_λ indicates that this control loop is now also used for tracking and not for increasing robustness. With this controller tuning the tracking error is reduced significantly compared to the results obtained in the previous scenarios.

Table 4. Case study 3: dry road

max. stability range		contr. setting		yaw rate	
U	$[15, 50]$	K_r	50000	$r^{(0)}$	0.29
μ_r	$[0.74, 1.36]$	$T_{\max}$	2000	$r^{(0)}_{\text{ref}}$	0.33
μ_l	$[0.74, 1.36]$	K_λ	100	r/r_{ref}	0.88

The third operating point considers only high values of μ around $\mu^{(0)} = 1.05$. The results in Table 4 show that in contrast to all previous results the specifications for the robust stability are not reflected in the controller settings. Even with all the controller parameters at their upper limits $K_r = 50000$, $T_{\max} = 2000$ and $K_\lambda = 100$, the distance to the nearest critical point is twice as large as the minimal distance specified by the desired ranges of the robustness region. For this point only the minimization of the tracking error is addressed, stability is fulfilled regardless of the parameter settings.

The robustness areas and critical manifolds around the three nominal operating points are depicted in Figure 5. These diagrams show that the stability boundary reaches further into the (μ_r, μ_l) plane with the tighter control tuning of the 2nd and 3rd operating point. the reduced robustness criteria can, however, be guaranteed for all three operating points.

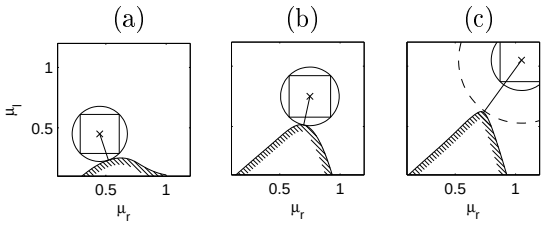

Fig. 5. Scenario 3: (a) icy road $\mu = (0.3, 0.6)$; (b) wet road $\mu = (0.6, 0.9)$; (c) dry road $\mu = (0.9, 1.2)$

5. CONCLUSIONS

The robust stabilization problem of a simple nonlinear vehicle model has been considered. The well known single-track model has been used for the vehicle dynamics and the performance of a simple proportional yaw rate feedback controller has been studied with respect to uncertainties in the vehicle longitudinal velocity, the hand wheel angle and the road adherence coefficients. For the control design constructive nonlinear dynamics have been used that ensure a lower bound on the parametric distance from the stability boundary. It has been shown that it is not possible to find a single tuning for the considered P-controller that stabilizes the complete range of uncertainty. The results of the gain scheduling in μ show that reduction of the tracking error and guaranteed stability are only possible for fairly good road conditions and reduced robustness ranges. For the icy road only the passive vehicle without yaw rate control could meet the requested robustness. An extension of the current study that includes the transient behavior of the vehicle states is currently under investigation.

REFERENCES

Ackermann, J., P. Blue, T. Bünte, L. Güvenc, D. Kaesbauer, M. Kordt, M. Muhler and D. Odenthal (2002). *Robust Control, The Parameter State Approach*. 2nd ed.. Springer Verlag. London.

Dobson, I. (1993). Computing a closest bifurcation instability in multidimensional parameter space. *Journal Nonlinear Science* **3**, 307–327.

Gustafsson, F. (1997). Slip-based tire-road friction estimation. *Automatica* **33**, 1087–1099.

Güvenç, B.A., T. Bünte, D. Odenthal and A. Güvenç (2004). Robust two degree-of-freedom vehicle steering controller design. *IEEE Transactions on Control Systems Technology* **12**(4), 627–636.

Mitschke, M. (1990). *Dynamik der Kraftfahrzeuge. Band C: Fahrverhalten*. 2nd ed.. Springer Verlag. Berlin.

Mönnigmann, M. and W. Marquardt (2002). Normal vectors on manifolds of critical points for parametric robustness of equilibrium solutions of ODE systems. *Journal of Nonlinear Science* **12**, 85–112.

Mönnigmann, M. and W. Marquardt (2003). Steady state process optimization with guaranteed robust stability and robust feasibility. *AIChE Journal* **49**, 3110–3126.

Ono, E. S. Hosoe and H.D. Tuan (1998). Bifurcation in vehicle dynamics and robust front wheel steering control. *IEEE Transactions on Control Systems Technology* **6**, 412–420.

Pacejka, H. B. and E. Bakker (1991). The magic formula tyre model. In: *1st International Colloqium on Tyre Models for Vehicle Dynamics Analysis*. Delft, the Netherlands.

Wiggins, S. (1990). *Introduction to Applied Nonlinear Dynamical Systems and Chaos*. Springer-Verlag. New York.